# Green's function Monte Carlo for few fermion problems

D. M. Arnow, M. H. Kalos, Michael A. Lee, and K. E. Schmidt

Citation: The Journal of Chemical Physics **77**, 5562 (1982); doi: 10.1063/1.443762
View online: http://dx.doi.org/10.1063/1.443762
View Table of Contents: http://scitation.aip.org/content/aip/journal/jcp/77/11?ver=pdfcov
Published by the AIP Publishing

# Green's function Monte Carlo for few fermion problems

D. M. Arnow,[a] M. H. Kalos, Michael A. Lee,[b] and K. E. Schmidt

*Courant Institute of Mathematical Sciences,[c] New York, New York 10012*
(Received 19 February 1982; accepted 27 August 1982)

The Green's function Monte Carlo method used for obtaining exact solutions to the Schrödinger equation of boson systems is generalized to treat systems of several fermions. We show that when it is possible to select eigenfunctions of the Hamiltonian based on physical symmetries, the GFMC method can be used to yield the lowest energy state of that symmetry. In particular, the lowest totally antisymmetric eigenfunction, the fermion ground state, can be obtained. Calculations on several two- and three-body model problems show the method to be computationally feasible for few-body systems.

## I. INTRODUCTION

Since its inception nearly two decades ago,[1] the Green's function Monte Carlo (GFMC) method has been a valuable tool in the study of quantum systems. First used by Kalos in the 1960's in the study of small nuclear systems,[1-4] the method, which yields exact numerical solutions to the Schrödinger equation, was generalized by Kalos, Levesque, and Verlet in 1974 to many-body problems in connection with their study of $^4$He.[5] The attractiveness of the method lies in the fact that it treats many-body problems exactly. The solutions which it yields have only a statistical sampling error, which can be accurately estimated and, in principle, made as small as desired. This can be accomplished either by increasing the size of the sample or by using the technique of importance sampling or both. This is in sharp contrast to variational calculations and other approximate methods. Since the results of a GFMC calculation have no error due to an approximation, such as a trial wave function, the method has been successfully used to make accurate comparisons between different potentials proposed for a given system.[6] It has also been used in comparing different trial functions in variational studies with a given potential.[7] Recently, efforts have been made to extend the GFMC method. Whitlock and Kalos have used GFMC to solve the Bloch equation in two-body finite temperature systems,[8] and Ceperley and Alder have used a version of the GFMC method to obtain approximate solutions to certain fermion problems.[9] Anderson, who has developed computational methods closely related to the GFMC method,[13,14] was, to our knowledge, the first to apply this class of methods to solving fermion problems.[15,16]

Unfortunately, the GFMC method, as mentioned above, will provide exact solutions only for bose systems; for reasons which will be explained later, in Sec. III B, no exact solutions can be obtained for fermi systems without substantial modifications of the GFMC method. Fermi systems are those systems where acceptable solutions to the Schrödinger equation are required to be anti-symmetric under interchange of identical particles. That is, if $i$ and $j$ are identical particles with the same spin, the wave function $\psi$ must have the property that

$$\psi(\ldots r_i \ldots r_j \ldots) = -\psi(\ldots r_j \ldots r_i \ldots). \tag{1.1}$$

Since most systems of physical interest are comprised of fermions, this leaves a large gap in many-body computational methods. Recent improvements in variational calculations for many-fermion systems[11] only heighten the need for a method for solving fermion problems that is equivalent to the GFMC method for bosons. It is the purpose of this paper to describe one such method, present results obtained from the method, and discuss its limitations.

The fermion Green's function Monte Carlo (FGFMC) method used here, like GFMC, rests upon the similarity between the Schrödinger equation and the time-independent diffusion equation. As in the GFMC method, a simulation of a diffusion process is carried out, with the diffusion governed by the inverse of the Hamiltonian operator, i.e., the Green's function. The potential part of the Hamiltonian is interpreted as an absorption process. To introduce antisymmetry into the solution, the simulations in FGFMC are carried out with two sets of points in configuration space, diffusing in a correlated fashion.

The next section of this paper describes the model problems selected for testing the new FGFMC method, and discusses the criteria for the selections. The third section explains the inherent difficulties in GFMC calculations for systems of fermions, outlines in detail the FGFMC algorithm, discusses a one-dimensional example of GFMC and FGFMC, and describes the way estimates for the energy are obtained, as well as other criteria for evaluating the success of the method. The fourth section presents the results obtained with the method for the given problems, and, in the final section some of the limitations of the algorithm are discussed, along with possible future avenues for improvement.

## II. THE MODEL PROBLEMS

Several criteria were used in selecting a suitable set of problems for developing the new FGFMC method. Since FGFMC is intended to be an exact method, at least some of the problems had to have known, ana-

[a]Current Address: Department of Computer and Information Science, Brooklyn College, C.U.N.Y. Brooklyn, New York, 11230.

[b]Current Address: Department of Physics, Kent State University, Kent, Ohio 44242.

[c]Supported by Grant ASO2-79ER 10353 from the U.S.D.O.E.

 021-9606/82/235562-11$02.10 

TABLE I. The model problems.

| | Potential I | | Potential II | | Potential III |
|---|---|---|---|---|---|
| | $V_2$ | $V_3$ | $V_2$ | $V_3$ | $V_2$ |
| $V_{rep}$[a] | 10.0 | 10.0 | 10.0 | 10.0 | 10.0 |
| $V_{wel}$[a] | −80.0 | −80.0 | −80.0 | −120.0 | −80.0 |
| $r_a$[b] | 1.0 | 1.0 | 4.0 | 1.0 | 2.0 |
| $r_b$[b] | 3.0 | 3.0 | 5.0 | 2.0 | 4.0 |
| $E_B$[a] | −95.598[d] | | −71.27 | | ...[c] |
| $E_F$[a] | −72.491 | | −66.907 | | ...[c] |

[a]The energy units are MeV.
[b]The units of distance are fermis.
[c]No exact, analytically known eigenvalue exists for this problem.
[d]In this potential, there is also an excited state, of energy −77.448, which is not antisymmetric.

lytical solutions for purposes of comparison. As will be shown later, our FGFMC is unfortunately sensitive to dimensionality; therefore a problem of extremely low dimension would not be appropriate for testing the algorithm's effectiveness, while a problem of high dimension might make initial explorations too difficult. Finally, it seemed necessary to use some problems in which there existed excited symmetric states of lower energy than the lowest antisymmetric state.

Accordingly, a system of three identical, spin 1/2 particles, each moving in three dimensions was selected. In all the work, it was assumed that particles 1 and 2 had like spin, differing from the spin of particle 3. Thus it was required that the spatial part of the ground fermion state can be antisymmetric upon interchange of particles 1 and 2. Three different central potentials were used. The first two were of the form

$$V^{I(II)}(R) = V_2(r_{12}) + V_3(r_{123}) , \tag{2.1}$$

differing only in the values of the parameters which define $V_2$ and $V_3$ [see Eq. (2.3) below and Table I], and the third of the form

$$V^{III}(R) = V_2(r_{12}) + V_2(r_{13}) + V_2(r_{23}) , \tag{2.2}$$

where $R = (r_1, r_2, r_3)$, $r_{ij} = r_i - r_j$, and $r_{123} = (r_1 + r_2)/2 - r_3$. $V_2$ and $V_3$ were both of the same form, square potentials with repulsive and attractive parts:

$$V_{2(3)}(r) = \begin{cases} V_{rep} > 0 \text{ if } r < r_a \\ V_{wel} < 0 \text{ if } r_a \le r_b \\ 0 \quad \text{if } r > r_b . \end{cases} \tag{2.3}$$

(See Fig. 1.) The values of the parameters ($r_a$, $r_b$, $V_{rep}$, $V_{wel}$) for the three potentials are summarized in Table I, along with the bose and fermion ground state energies ($E_B$ and $E_F$). The different potentials were used to ensure the existence of excited symmetric states lower than the ground antisymmetric state in some of the problems. For the first two potentials, analytical solutions can be constructed, while for the third potential, very good variational trial functions are available.

## III. THE FGFMC METHOD

### A. The GFMC method

The standard GFMC method, as employed in numerical solutions of bose problems, is described in detail elsewhere.[5,10,12] We will thus only describe it in the rudimentary form necessary to develop the subsequent formalism. We begin with the $N$-body Schrödinger equation for identical particles

$$[-\nabla_R^2 + V(R)]\psi_n(R) = E_n \psi_n(R) . \tag{3.1}$$

Here $R$ represents the $3N$ coordinates of all particles, $R = (r_1, \ldots, r_n)$ and $V$ may be potential which, for simplicity, we assume positive in what follows.

This may be rewritten in its integral form

$$\psi_n(R) = E_n \int G(R, R')\, \psi_n(R')\, dR' . \tag{3.2}$$

where $G(R, R')$, the Green's function, satisfies the equation

$$HG(R, R') = \delta(R - R') , \tag{3.3}$$

and the boundary conditions of the problem, namely that $G \to 0$ as $|r_i - r_j| \to \infty$. The Neumann series solution to the integral equation is

$$\psi^{(n)}(R) = E_B \int G(R, R')\, \psi^{(n-1)}(R')\, dR' \tag{3.4}$$

and $\psi^{(n)}(R) \to \psi_B(R)$, the Bose ground state, as $n \to \infty$, provided that $\langle \psi_B | \psi^{(0)} \rangle \neq 0$. The convergence is geometric in the sense that $\langle \psi_m | \psi^{(n)} \rangle$ decreases geometrically with ratio $E_B/E_m$, for large $n$. It is desirable to explain what is meant by a Monte Carlo "solution" for the function $\psi$. Such a solution consists of a set of points $S = \{R_i\}$ distributed in $3N$ space with probability density $\psi \ge 0$, i.e., sampled from $\psi$. The function $\psi$ may now be considered known in the sense that the integral of $\psi$ with any other function $f$ is given by

$$\frac{\int \psi(R) f(R)\, dR}{\int \psi(R)\, dR} \simeq \sum_{i=1}^{M} f(R_i) ,$$

where $M$ is the number of points $R_i$ in set $S$ and the approximation is in the usual sense of Monte Carlo.

For Bose systems one begins with an initial set of

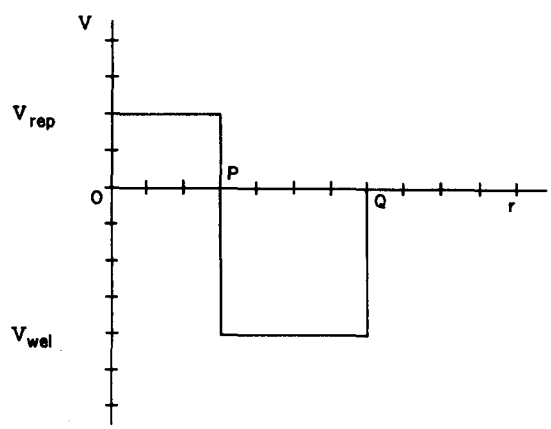


FIG. 1. The form of the potentials in the model problems.

points obtained from an analytically known trial wave function $\psi^{(0)}$, selected along with a trial energy $E_T$. The assumption here, that $\psi^{(0)}$ be non-negative everywhere is satisfied by the Bose ground state.

For each point $R_j$, a new set of points is sampled from the density function $E_T G(R, R_j)$. The union of all new sets constitutes the set of points representing the wave function of the next stage of iteration $\psi^{(1)}$. Since $E_T G(R, R_j)$ is not of unit norm, the population of points may grow or decline. The ratio of such change at each iteration is asymptocially geometric with ratio $E_T/E_B$, providing a means of estimating the energy $E_B$, the so-called "growth estimator". The crux of the problem lies in constructing a method for sampling $G(R, R')$, which is not known in general but which satisfies

$$[-\nabla_R^2 + V(R)]G(R, R') = \delta(R - R') \ . \tag{3.5}$$

Choosing some $U > V(R)$, may construct another Green's function $G_U(R, R'')$, which satisfies

$$[\nabla_R^2 + U]G_U(R, R'') = \delta(R - R'') \ . \tag{3.6}$$

In the work described below, we used solutions of Eq. (3.6) defined over all space. Multiplying Eq. (3.5) by $G_U(R, R'')$, Eq. (3.6) by $G(R, R')$, integrating both over $R$ and subtracting yields

$$\begin{aligned} G(R', R'') &= G_U(R, R'') + \int \left[\frac{U - V(R)}{U}\right] U G_U(R, R'') G(R', R'') dR \\ &+ \int [G_U(R, R'')\nabla_R^2 G(R, R') - G(R, R')\nabla_R^2 G_U(R, R'')] dR \\ &= G_U(R', R'') + \int \left[\frac{U - V(R)}{U}\right] U G_U(R, R'') G(R', R) dR \ , \end{aligned} \tag{3.7}$$

using Green's theorem. The iteration of this equation gives $G$ as an infinite series involving only $G_U$. This iterative process is used to define a random walk which then samples $G$. Given a point $R''$, to sample a point $R'$ from $G(R', R'')$, three steps are necessary. First, $G_U(R', R'')$ is sampled, generating a set of points $g_1$. Then, from $UG_U(R, R'')$, a point $R$ is sampled, with probability $[U - V(R)]/U$. From this point $R$ more points are to be sampled with $G(R', R)$ as the density function generating a set of points $g_2$. The stochastic process continues until the continuation probability $[U - V(R)]/U$ forces a termination. The union of the sets $g_i$ is then distributed according to $G(R', R'')$.

### B. Obstacles presented by Fermi statistics

Difficulties are encountered immediately upon trying to use the above method to obtain antisymmetric ground state solutions. Such a solution inevitably is both positive valued and negative valued and cannot be used as a density function. Also, as indicated above, the GFMC iteration always converges geometrically to the lowest, generally symmetric, state. Furthermore, even if it were possible to prevent convergence to the lowest state, in most problems of interest there exist many excited states of lower energy than the antisymmetric ground state. From another point of view, the algorithm depends solely on the Schrödinger equation and the boundary conditions, neither of which contains any information about the antisymmetry.

To overcome the first difficulty, the amtisymmetric wave function $\psi_F(R)$ is rewritten as the difference of two non-negative functions

$$\psi_F(R) = \psi^+(R) - \psi^-(R) \ . \tag{3.8}$$

Substituting $\psi^+$ and $\psi^-$ into the integral Eq. (3.2), we have

$$\psi^+(R^+) = E_F \int G(R^+, R^{+\prime})\psi^+(R^{+\prime}) dR^{+\prime} \ , \tag{3.9a}$$

$$\psi^-(R^-) = E_F \int G(R^-, R^{-\prime})\psi^-(R^{-\prime}) dR^{-\prime} \ . \tag{3.9b}$$

Equations (3.9a) and (3.9b) suggest that two distinct populations, representing $\psi^+$ and $\psi^-$, be iterated independently. This approach leads to gross inefficiency for two reasons. First, the overlap of $\psi^\pm$ with the ground state ($\psi_0$) is not zero, hence separate iteration will inevitably result in $\psi^+$ and $\psi^-$ separately converging to the bose ground state. Secondly, Monte Carlo deals with sets of points and there is no way of subtracting two sets of points, as one would subtract analytic $\psi^\pm$. This problem is most easily understood if we consider a system with only two important low lying states, the bose and fermi ground states. At every iteration the $\psi^\pm$ is dominated by two terms

$$\begin{aligned} \psi^+(R) &= \alpha_B \psi_B + \tfrac{1}{2}\psi_F(R) \ , \\ \psi^-(R) &= \alpha_B \psi_B - \tfrac{1}{2}\psi_F(R) \ , \\ \psi_F(R) &= \psi^+ - \psi^- \ , \end{aligned}$$

where $\psi_B$ is the lowest symmetric state and where $\alpha_B$ is large enough to ensure that $\psi^+$ and $\psi^-$ are positive or zero everywhere.

As Eq. (3.4) is repeatedly applied, $\alpha_B$ increases geometrically with ratio $(E_F/E_B)$, i.e., the symmetric component of $\psi^+$ and $\psi^-$ grows relative to the antisymmetric component. Although this does not bias the computation, since $\psi_F = \psi^+ - \psi^-$ independently of $\alpha_B$, the standard error of the calculation increases dramatically.

All quantities that are calculated from the populations generated by FGFMC can be related to sums of the form

$$Q = \sum_j A(R_j^+) - \sum_j A(R_j^-) \ , \tag{3.10}$$

where $A$ is some antisymmetric function and where $\{R_j^+\}$ and $\{R_j^-\}$ are distributed with density $\psi^+$ and $\psi^-$ respectively. The expectation for such a sum is proportional to

$$\int A(R)\psi^+(R) dR - \int A(R)\psi^-(R) dR \ , \tag{3.11}$$

and is independent of the symmetric components of $\psi^+$ and $\psi^-$, since the integral of the product of an antisymmetric function and a symmetric function is zero. However, the variance of $Q$ includes terms proportional to

$$\int (A(R))^2 \psi^+(R) dR \ , \tag{3.12}$$

which increase with greater symmetric component, since $A(R)^2$ is a symmetric function. Thus, the geometric growth of the symmetric component in $\psi^+$ and $\psi^-$

leads to an exponential growth in variance, relative to average value. Such a situation is unacceptable.

Even though the method described thus far fails to produce an exact fermion solution, it is not without utility. An analagous procedure was successfully applied in calculations on the ground state of $^3$He and the electron gas.[9,17]

### C. Pair Green's functions

To avoid the above mentioned difficulties we begin by defining a pair Green's function[18]:

$$G^{\pm}(R;R^+,R^-)=G(R,R^+)-G(R,R^-)\ . \tag{3.13}$$

The Monte Carlo sums which correspond to Eqs. (3.9a) and (3.9b) are

$$\psi^+(R^+)=\sum_j E_F G(R^+,R_j^{+\prime}) \tag{3.14a}$$

and

$$\psi^-(R^-)=\sum_j E_F G(R^-,R_j^{-\prime})\ , \tag{3.14b}$$

where the sums are take over sets of points $\{R^+\}$ and $\{R^-\}$ which have been constructed by sampling $\psi^+$ and $\psi^-$, respectively. By adding Eqs. (3.14a) and (3.14b) and substituting Eq. (3.13) into the result, one obtains

$$\psi^+(R^+)+\psi^-(R^-)=E_F\sum_j G^{\pm}(R;R_j^+,R_j^-)\ . \tag{3.16}$$

The implication here is that pairs of points $(R^+,R^-)$ are selected from the sets representing $\psi^+$ and $\psi^-$ in the current step of the process. Wherever $G^{\pm}>0$, the sampled point $R$ is considered to be an $R^+$ point, representing $\psi^+$ in the next step; otherwise it becomes an $R^-$ point, representing $\psi^-$. Because sums such as

$$\sum_j G(R,R_j^+)-\sum_j G(R,R_j^-)\ , \tag{3.17}$$

where $R_j^+$ and $R_j^-$ are sampled from $\psi^+$ and $\psi^-$, are independent of the order of selection of $R_j^+$ and $R_j^-$, the particular choice made for pairing points does not bias the computation. If $G$, and thus $G^{\pm}$ is unknown, the latter can be sampled by defining $G_U^{\pm}(R;R^+,R^-)$,

$$G_U^{\pm}(R;R^+,R^-)=G_U(R,R^+)-G_U(R,R^-)\ , \tag{3.18}$$

and using the integral equation

$$\begin{aligned}G^{\pm}(R;R^+,R^-)&=G_U^{\pm}(R;R^+,R^-)\\&+\int\left[\frac{U-V(R^{+\prime\prime})}{U}\right]UG_U(R^{+\prime\prime},R^{+\prime})G(R,R^{+\prime\prime})dR^{+\prime\prime}\\&-\int\left[\frac{U-V(R^{-\prime\prime})}{U}\right]UG_U(R^{-\prime\prime},R^{-\prime})G(R,R^{-\prime\prime})dR^{-\prime\prime}.\end{aligned} \tag{3.19}$$

The advantage of using $G^+$ lies in the fact that a substantial part of the subtraction of $\psi^+-\psi^-$ is contained in $G^{\pm}$ rather than represented by the "subtraction" of sets of points. A measure of how much subtraction has been incorporated into $G^{\pm}$ is

$$\sum_j\int[G(R,R_j^+)+G(R,R_j^-)]dR-\int|G^{\pm}(R;R_j^+,R_j^-)|dR. \tag{3.20}$$

This quantity is greatest when $R_j^+$ and $R_j^-$ are close. Hence the efficiency of the reduction of the symmetric component will depend on the size of population and on the manner in which points are paired. Clearly there exists some optimal pairing, of points $R^+$ to $R^-$ to maximize this quantity over the entire iteration. To generate such a pairing is not a trivial operation since, during each step of the iteration, the set of points is not only being depleted but also is gaining new points in the course of sampling $G$ with $G_U$. Our solution to the problem (in 9 dimensions) has been to select, for a given $R^+$, the nearest $R^-$ within a small set of cubes centered about $R^+$. In a similar fashion, $R^+$ points are paired with $R^-$ points. Although this scheme does not result in an optimal pairing, let alone in the pairing of nearest neighbors, it has proved sufficiently effective in maximizing the condition of Eq. (3.20) to make the overall algorithm work.

To summarize the FGFMC method used here, two sets of points representing $\psi^{+(0)}$ and $\psi^{-(0)}$ are initially sampled. In each iteration, pairs of points $(R^+,R^-)$, one from each set, are removed from the sets and new points for the next generation are sampled from $|G^{\pm}(R;R^+,R^-)|$. Where $G^{\pm}>0$, the new points are taken to represent $\psi^+$, otherwise they represent $\psi^-$. $G^{\pm}$ is sampled by moving points in a random walk governed by Eq. (3.19). Points are sampled from $UG_U(R,R')$ and with probability $[U-V(R)]/U$ added to the current sets of points representing $\psi^+$ or $\psi^-$. Eventually, the current sets of points are exhausted and another iteration is made.

### D. An illustrative example

The ideas of the previous section were first tested with exactly solvable two particle systems. It is instructive to consider one such simple example, where the interparticle potential confines the two particles to be within a fixed radius. Such problems reduce to one body problems and we will illustrate this by considering the simplest case possible, the particle in a box.

The eigenfunctions of the Hamiltonian for a particle restricted to an interval $(-\pi,\pi)$, and the Green's function are well known.

$$\psi_n(x)=\pi^{-1/2}\cos\left(\frac{nx}{2}\right)\ \text{for}\ n=1,3,5,\ldots$$

$$=\pi^{-1/2}\sin\ (nx/2)\ \text{for}\ n=2,4,6,\ldots$$

and

$$G(x,x')=\frac{(x+\pi)(\pi-x')}{2\pi}\ \text{for}\ x<x'\ ,$$

$$G(x,x')=\frac{(x-\pi)(-\pi-x')}{2\pi}\ \text{for}\ x>x'\ .$$

In order to make a plausible demonstration of the FGFMC method, we will not employ our knowledge of the nodes of the fermion wave function in this problem.

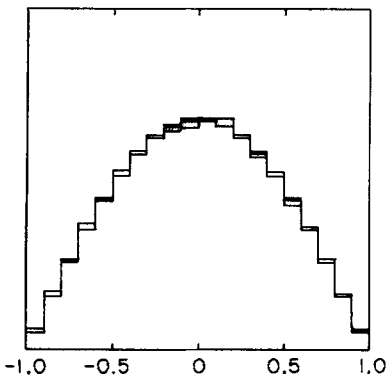


FIG. 2. GFMC solution for a single particle in a box after ten interations (2000 points per iteration) compared with analytical solution.

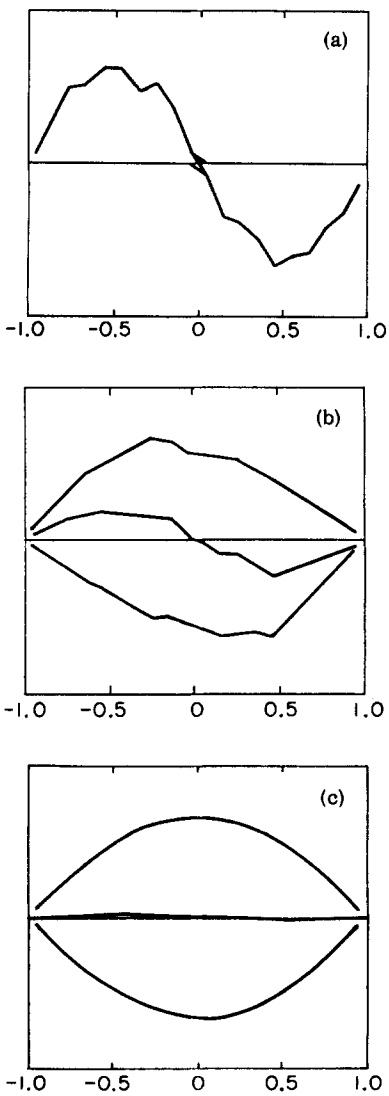


FIG. 3. (a) The distribution of an initial population (and its antisymmetric component) drawn from the analytical solution to the first excited state of the particle in a box. (b) The distribution of the population (and its antisymmetric component) after 5 iterations of naively applying GFMC to the population in Fig. 3(a). (c) The distribution of the population (and its antisymmetric component) after 50 iterations of naively applying GFMC to the population in Fig. 3(a).

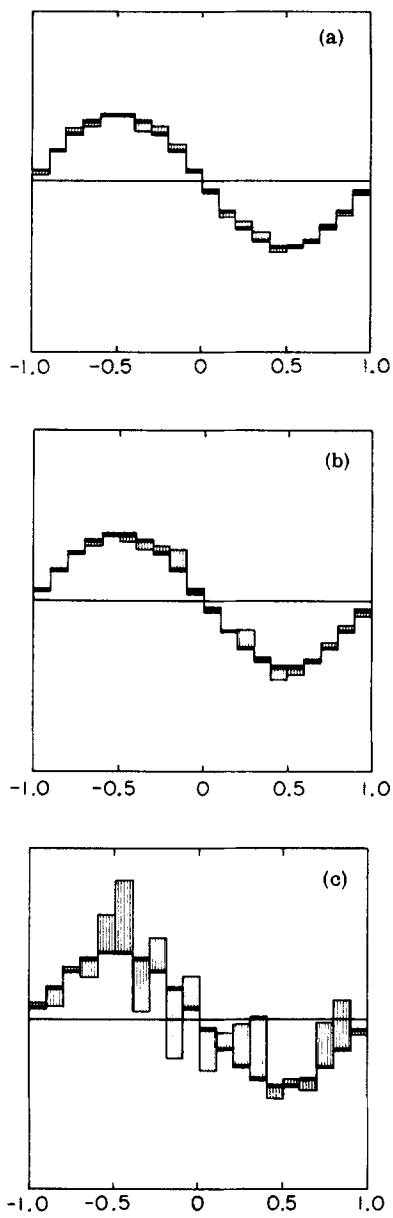


FIG. 4. (a) A comparison of the analytical first excited state with the population shown in Fig. 3(a). (b) A comparison of the analytical first excited state with the population shown in Fig. 3(b). (c) A comparison of the analytical first excited state with the population shown in Fig. 3(c).

As described above we begin with a set of points distributed according to an initial trial function $\psi^{(0)}$. We commence the iteration by sampling points $x$ from $G(x, x')$ for each $x'$ in the set representing $\psi^{(0)}$. These new points are then used to generate more points by successively sampling $G$. Eventually, one obtains a set of points which statistically represent the ground state wave function $\cos(x)$. A program based on this procedure generated, after ten iterations (with 2000 points per iteration), the histograms shown in Fig. 2. For comparison, histograms computed from the analytically known wave function are also displayed. We have chosen to present a case with noticeable statistical fluctuations, for illustrative purposes.

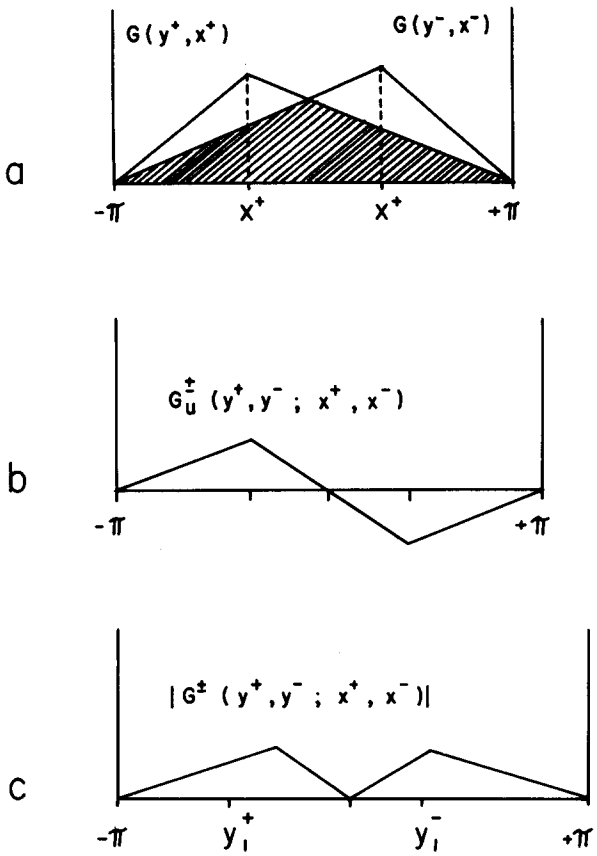


FIG. 5. The FGFMC procedure.

If the above procedure is applied independently to two sets of points representing $\psi^+$ and $\psi^-$ [as suggested by Eqs. (3.9a) and (3.9b)], then, even starting with an excellent initial population, the antisymmetric component declines and the error of the generated wave function increases sharply. A program following this procedure started with an initial population drawn from the analytically known solution itself [$\sin(x)$]. It and its antisymmetric component are plotted in Figs. 3(a) and 4(a). Figures 3(b) and 4(b) show the wave function after five iterations (after which there is little but noise in the populations), and Figs. 3(c) and 4(c) show it after 50 iterations.

An effective procedure for obtaining the first excited state, the antisymmetric fermion state $\sin(x)$ modifies the above, ineffective procedure to incorporate the pair Green's function operating on two sets of points. Figure 5 illustrates the Monte Carlo process suggested by Eq. (3.16).

### *Procedure*

(1). Given two populations, representing $\psi^{+(n)}$ and $\psi^{-(n)}$ at the $n$th iteration, select a pair $x^+, x^-$, and construct their respective Green's functions. [See Fig. 5(a).]

(2). Construct $G^{\pm}(y^+, y^-; x^+, x^-)$ by subtracting the individual Green's functions and sample $y^+$ and $y^-$ from the positive and negative regions respectively. [See Fig. 5(b).]

(3). Accept the new pair (i.e., add it to the sets of the next generation of points) with a weight of one-half of the integral of the absolute value of the Green's function $G^{\pm}$. [See Fig. 5(c).] The greater the degree of overlap between the two individual Green's functions, the smaller the probability of accepting the new pair. If this quantity is less than half the sum of the integrals of each of the two individual Green's functions, then the pairing has decreased the probability of the acceptance of the new pair.

A calculation based on this procedure was performed with an initial population of randomly distributed, symmetric noise (with *no antisymmetric component*). Plots of the antisymmetric component of the population are shown in Figs. 6(a), 6(b), and 6(c) for 0, 5, and 10 iterations. A histogram, comparing the Monte Carlo

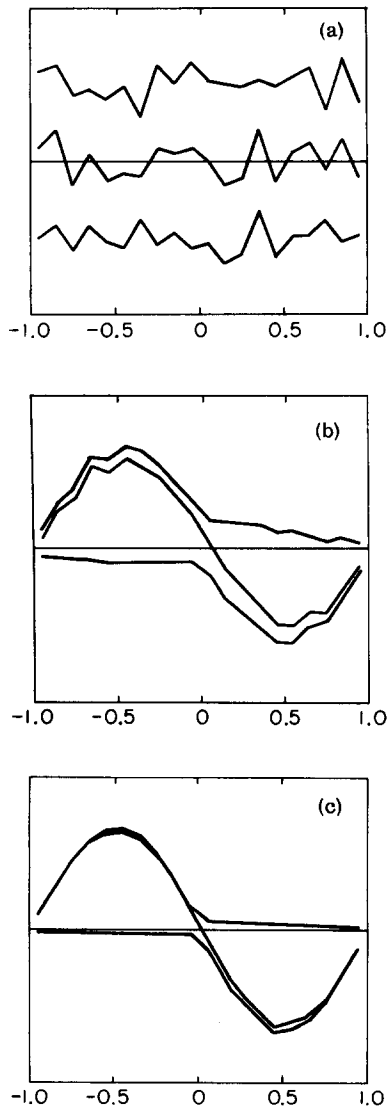


FIG. 6. (a) The uniform, random distribution of an initial population (and its antisymmetric component). (b) The distribution of the population after five iterations of applying the FGFMC procedure to the population in Fig. 6(a). (c) The distribution of the population (an its antisymmetric component) after ten iterations of applying the FGFMC procedure to the population shown in Fig. 6(a).

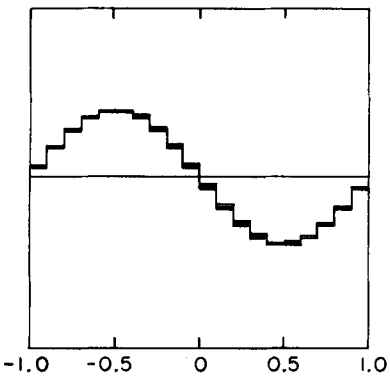


FIG. 7. A comparison of the analytical first excited state with the population generated by FGFMC procedure from pure noise after ten iterations [also shown in Fig. 6(c)].

generated function with the true wave function, $\sin(x)$, is shown in Fig. 7. The histogram and the plots demonstrate the ability of the method to start from a worst case (symmetric noise) and successfully produce the antisymmetric state.

There is no question that the procedure described above is correct, but these examples serve to illustrate the statistical nature of the method. The efficiency of the procedure is then the critical consideration, in particular, its dependence on the size of the populations and the number of particles. Further analysis and discussion of these points will be left until the results of the three-body problems are presented.

### E. Excited symmetric states

The above method of using $G^{\pm}$ is adequate for increasing the antisymmetric component in the populations. However, the correct wave function is not antisymmetric under interchange of any two particles, only under interchange of those which are identical fermions of equal spin. If the method includes no means for utilizing information identifying such pairs, then the populations generated may include as components, states which have positive and negative values (and thus nodes) and yet which are symmetric upon interchange of particles which are identical fermions of equal spin, provided that these states are of lower energy than the lowest fermion state. Such states are excited symmetric states, and are undesirable for the reasons outlined in Sec. III B above.

To avoid this difficulty (which does not arise in the one-dimensional case), the algorithm was modified so that if $(\ldots r_i, \ldots r_j, \ldots)$ was an $R^+$ point where $i$ and $j$ identify identical fermions of equal spin then $(\ldots, r_j, \ldots, r_i, \ldots)$ was added as an $R^-$ point. In our calculations, that measure alone was enough to prevent the development of excited symmetric components in the populations. If needed, an additional feature could have been added to the algorithm. If $(\ldots, r_i, \ldots r_j, \ldots)$ was an $R^+$ point where $i$ and $j$ identify particles (which are *not* identical fermions of equal spin) then $(\ldots, r_i, \ldots, r_j, \ldots)$ could be added as an $R^-$ point.

### F. Estimation of the energy

The GFMC algorithm itself automatically provides an estimate of the energy based on changes in population size from one iteration to the next. Such an estimate is called a "growth estimate" and is discussed at some length in Eq. (10). If $N_m$ represents the population size at the $m$th iteration, then a growth estimate at the $(m+1)$th iteration is

$$E_F = \frac{(E_T - V_0)N_m}{N_{m+1}} - V_0 , \tag{3.21}$$

where $E_T$ is the trial energy and $V_0$ is the rescaling constant of the energy scale. This estimator has a number of biases which are discussed in Eq. (10).

In the current algorithm, such an estimator is not valid because what is required to estimate the fermion energy is the ratio of growth of the antisymmetric component of the population, not the growth of the entire population. A valid growth estimator then is

$$E_F = (E_T + V_0)\frac{\sum_j A(R_j^+) - \sum_j A(R_j^-)}{\sum_h A(R_k^{+\prime}) - \sum_k A(R_k^{-\prime})} - V_0 , \tag{3.22}$$

where $R_j^+$ and $R_j^-$ are the populations sampled at the $m$th iteration, $R_k^{+\prime}$ and $R_k^{-\prime}$ are the populations sampled at the $(m+1)$th iteration, and where $A$ is any antisymmetric function which is not orthogonal to the true wave function. Because of the antisymmetric nature of $A$, the symmetric component in $\psi^+$ and $\psi^-$ will tend to cancel out in both numerator and denominator, leaving only the antisymmetric component. It should be noted that the variance of the estimator decreases as the inner product of $A$ with the true wave function increases.

A less biased and more efficient estimator for the energy is the "mixed estimator", so called because it "mixes" the GFMC technique with the use of variational trial functions. With an antisymmetric trial function labeled as $\psi_T(R)$, one can multiply the Schrödinger equation by $\psi_T(R)$ and integrate over $R$ space to yield

$$E_F = \frac{\langle \psi_T | H | \psi_F \rangle}{\langle \psi_T | \psi_F \rangle} = \frac{\langle \psi_F | H | \psi_T \rangle}{\langle \psi_F | \psi_T \rangle} , \tag{3.23}$$

where $\psi_F$ is the lowest antisymmetric eigenfunction of the Hamiltonian. An estimate of $E_F$ based on a set of points $\{R_j\}$ sampled from $\psi_F$ can be made as

$$E_F = \frac{\sum_j H\psi_T(R_j)}{\sum_j \psi_T(R_j)} . \tag{3.24}$$

The estimate is valid since the symmetric components of $\psi_F$ cancel out since $\psi_T$ is antisymmetric. It should be pointed out that the expectation of the quotient of sums here is $E_F$ if $\psi_F$ has converged, regardless of the character (other than antisymmetry) of $\psi_T$, i.e., the estimate is exact, having no variational error; the variance, however, will go to zero as $\psi_T$ becomes closer to the true fermion ground state wave function since

$$\frac{H\psi_T(R)}{\psi_T(R)} \to \frac{E_F\psi_F(R)}{\psi_F(R)} = E_F , \tag{3.25}$$

as $\psi_T \to \psi_F$ independently of $R$.

TABLE II. The mixed estimator trial functions.

| | Potential I | | Potential II | | Potential III | |
|---|---|---|---|---|---|---|
| Trial function[a] | $\Psi_A^I$ | $\Psi_B^I$ | $\Psi_A^{II}$ | $\Psi_B^{II}$ | $\Psi_A^{III}$ | $\Psi_B^{III}$ |
| Variational energy[b] | −68.7 | −26.0 | −56.0 | −26.0 | −134.0 | −74.0 |
| Mixed estimate on a random set[c] | −103.0 | −126.0 | −106.0 | −122.0 | −141.0 | −102.0 |
| Exact energy | −72.491 | | −66.906 | | ... | |

[a]Defined in Eqs. (4.1), (4.2), (4.3), and (4.4).
[b]The variational integral was calculated by using the Metropolis Monte Carlo algorithm.
[c]Using the trial function as a mixed estimator function (3.24) with a populations of points that are distributed uniformly, randomly and, on the average, symmetrically within the region of space of lowest potential, rather than with a population generated by FGFMC.

### G. The ground state wave function

In addition to computing various estimates of the ground state energy, a number of quantities were calculated which served to check the convergence of the populations to the fermion ground state wave function.

First, the mean points of the populations representing $\psi^+$ and $\psi^-$ were computed. The norm of the vector difference between these two points $|R_D|$ was then calculated. This provided a test of the effectiveness of $G^*$. If both populations converged to the ground boson state (as would happen without $G^*$, or if the $R^+$ and $R^-$ points were not paired sufficiently close to each other), $|R_D|$ would go to zero. For $|R_D|$ to converge to a number significantly greater than zero would mean that the populations representing $\psi^+$ and $\psi^-$ were, to an extent, occupying disjoint regions of space. This would be the case if the populations were representing a fermion state; it would also be the case if they were representing an excited bose state. Thus, while useful, $|R_D|$ was not sufficient in proving the desired convergence.

Secondly, the quantities

$$p_i = \int_{z_i}^{z_{i+1}} \int\int\int\int \psi_F(R) dR_{CM}\, dr_{123}\, dx_{12}\, dy_{12}\, dz_{12} \qquad (3.26)$$

were estimated by constructing a histogram along the $z_{12}$ axis. In effect, then, the projection of the population of points on the $z_{12}$ axis was estimated. Weights of +1 were assigned to points representing $\psi^+$ and weights −1 were assigned to those representing $\psi^-$, and the points were then assigned to bins according to their $z_{12}$ value. Summing up the absolute values of such a histogram and dividing by the total population size yields a quantity $f$, which indicates the fraction of points which are representing the ground fermion state. If the algorithm was incorrect, $f$ would be close to zero; if the algorithm was perfect, $f$ would be 1. Even if $f$ is less than 1, the algorithm may well be effective. In a calculation of any quantity of interest ($E_F$ for example), those points representing the symmetric component will tend to cancel out. The important point is that $f$ should be stable over the course of the iterations. Such stability indicates that the growth of the symmetric component truly has been arrested.

Finally, a measure of the overlap of $\psi_F$ with $\psi_T$ can be computed from

$$P = \frac{|\sum_j \psi_T(R_j^+) - \sum_j \psi_T(R_j^-)|}{(\text{population size})}\,, \qquad (3.27)$$

with $R_j^+$ taken from $\psi^+$ and $R_j^-$ from $\psi^-$. When $\psi^+$ and $\psi^-$ are dominated by symmetric component, $P$ will tend to zero. $P$ may be very high if excited fermion states are present, but as this is unlikely (in view of the nature of GFMC calculations) after a few iterations, a high value of $P$ may be taken to mean effectiveness of the algorithm. Regardless of the value of $P$, stability of $P$ indicates the success of the algorithm in maintaining the correct antisymmetric component. If the procedure converges to a state that is not antisymmetric then $P$ converges to zero.

## IV. RESULTS

For each model problem, two mixed energy estimates were made [Eq. (3.24)]. To obtain such estimates for model problem I (II), the trial function

$$\Psi_A^{I(II)}(R) = \psi_1(r_{12})\,\psi_0(r_{123}) \qquad (4.1)$$

was employed, where $\psi_1$ is the first excited state solution for a single particle $r_{12}$ in a potential identical to that given by the $V_2$ term in potential I (II) (see Table I) but for a slight modification of the parameters defining the potential, and where $\psi_0$ is the lowest state solution for a single particle $r_{123}$ in a potential identical to that given by the $V_3$ term in potential I (II) but for a slight modification of the parameters defining the potential. Another trial function of similar form was also used,

$$\Psi_B^{I(II)}(R) = \psi_1'(r_{12})\,\psi_0'(r_{123})\,, \qquad (4.2)$$

where $\psi_1'$ and $\psi_0'$ are, in this case, solutions for single particles in potentials considerably different from those given by the $V_2$ and $V_3$ terms in potential I (II). The variational energies given by the trial functions are presented in Table II. The reason for using two trial functions to obtain two mixed estimates for each problem was to test the concentration, made earlier in Sec. III, that only the variance and not the expectation of the energy estimate is effected by the quality of the variational trial function. As can be seen from Table

TABLE III. FGFMC energy estimates.

| | Potential I | Potential II | Potential III |
|---|---|---|---|
| Exact energy | −72.491 | −66.906 | ...[a] |
| Growth estimate | −74.4 ± 1.6 | −66.7 ± 0.9 | −138.6 ± 1.0 |
| Mixed estimate (*A*) | −72.8 ± 0.4[b] | −66.9 ± 0.5[b] | −138.25 ± 0.16[c] |
| Mixed estimate (*B*) | −73.4 ± 1.3[d] | −67.0 ± 0.9[d] | −138.4 ± 1.0[e] |

[a]Not available.
[b]Produced with the mixed estimator function $\Psi_A^{\mathrm{I}}$ or $\Psi_A^{\mathrm{II}}$ given by the Eq. (4.1).
[c]Produced with the mixed estimator function $\Psi_A^{\mathrm{III}}$ given by Eq. (4.3).
[d]Produced with the mixed estimator function $\Psi_B^{\mathrm{I}}$ or $\Psi_B^{\mathrm{II}}$ given by Eq. (4.2).
[e]Produced with the mixed estimator function $\Psi_B^{\mathrm{III}}$ given by Eq. (4.4).

II, the functions $\psi_A$ and $\psi_B$ are qualitatively very different trial functions.

Similarly, for model problem III, two trial functions were used, a good one

$$\Psi_A^{\mathrm{I(II)}}(R) = \psi_1(r_{12})\,\psi_0(r_{13})\,\psi_0(r_{23})\,, \tag{4.3}$$

where $\psi_1$ and $\psi_0$ are the first excited state and ground state solutions for a single particle $r_{12}, r_{13}$, or $r_{23}$ in a potential given by the $V_2$ term in potential III, as well as a relatively poor trial function

$$\Psi_B^{\mathrm{III}}(R) = \psi_1'(r_{12})\,\psi_0'(r_{13})\,\psi_0'(r_{23})\,, \tag{4.4}$$

where $\psi_1'$ and $\psi_0'$ are solutions for a single particle in potentials quite different from that given by the $V_2$ term in potential III. The variational energies given by these functions are shown in Table II.

In addition to the two mixed estimates of the energy for each of the problems, a growth estimate was made as well. The results of all these estimates are given in Table III. These results demonstrate the reliability of all the estimates, the superiority of the mixed estimator to the growth estimator, and the advantage of using a better trial function over an inferior one (the third and fourth rows of Table III respectively). To indicate how much of the success of these estimates is due to the quality of the trial functions and how much is due to the quality of the FGFMC generated population on which these estimates were based, the final row of Table III indicates the results of applying the mixed estimator to sets of points uniformly and randomly distributed in the region of space which has the lowest potential. The fact that for the inferior trial functions the energies calculated with such populations are very far from correct, while using the same functions with FGFMC generated population yields the correct energy is strong evidence for the effectiveness of the FGFMC method. On the other hand, the fact that the energies calculated with the superior trial functions and with random populations are relatively close to the correct energies demonstrates the advantage to be gained by using good variational trial functions (which are generally available for most physical systems) in an FGFMC calculation.

Table IV lists the values of $|R_D|$, $f$, and $P$, defined in the previous section, which indicate the character of the FGFMC-generated wave function. The overlaps $P$ were calculated using the optimal variational function in each case. For each potential, these values are given for the starting population, a set of points uniformly and randomly distributed in the region of space with the lowest potential, at iteration 0, iteration 10, iteration 30, and at convergence (around 70). The initial growth of these quantities and their subsequent stability indicates the success of the method. It should be noted that these iterations represent a worst case situation, since normally an FGFMC calculation would be started from a population sampled from a fairly good variational trial function, not from a uniform, symmetric distribution. That the FGFMC algorithm generated, in each case, populations of points with the correct antisymmetry, having started with an initial population which not only did not have the right antisymmetry but which was symmetric on the average, is a remarkable testimonial to the algorithm's effectiveness.

Figures 8(a) and 8(b) compare the projection of the FGFMC generated wave function onto the $z_{12}$ axis with that of the true one. The close agreement is indicative of the correctness of the algorithm.

Each FGFMC iteration requires 15 VAX cpu minutes, excluding the time necessary to calculate the estimates and other quantities.

## V. CONCLUSIONS

An exact Green's function Monte Carlo method has been developed for the fermion problem. The power of the method is demonstrated by its ability to start with

TABLE IV. FGFMC convergence.

| | Potential I | | | Potential II | | | Potential III | | |
|---|---|---|---|---|---|---|---|---|---|
| Steps | $f$[a] | $R_D$[b] | $P$[c] | $f$ | $R_D$ | $P$ | $f$ | $R_D$ | $P$ |
| 0 | 0.09 | 0.29 | 0.15 | 0.09 | 0.29 | 0.13 | 0.12 | 0.29 | 0.02 |
| 10 | 0.19 | 0.84 | 1.49 | ... | 2.70 | 0.32 | 0.22 | 0.86 | 0.13 |
| 30 | 0.14 | 0.64 | 1.38 | 0.80 | 4.70 | 0.62 | ... | 2.30 | 0.53 |
| Convergence | 0.37 | 1.74 | 2.83 | 0.78 | 5.83 | 5.73 | 0.59 | 2.84 | 3.14 |

[a]Defined by Eq. (3.26) and subsequent discussion.
[b]Defined in the discussion in Sec. III D.
[c]Defined by Eq. (3.27).

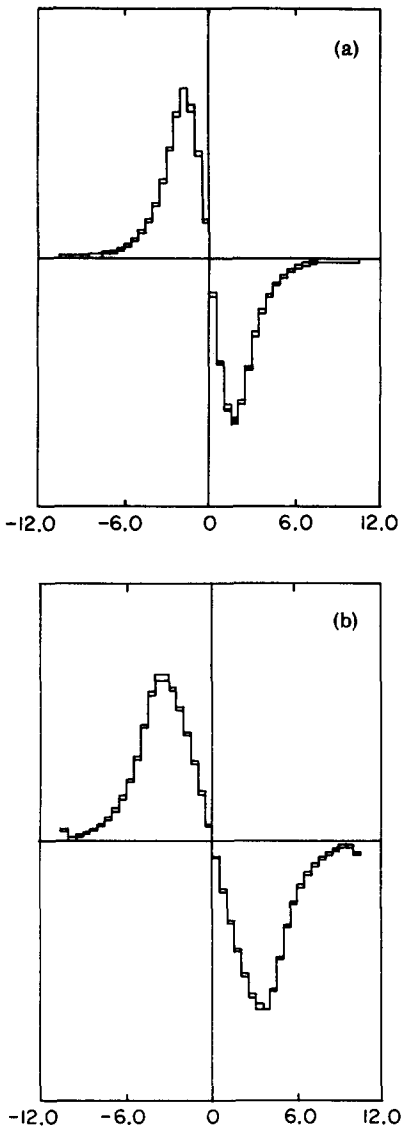


FIG. 8. (a) The nine-dimensional problem; the projection of the FGFMC generated wave function (for model problem I) onto the $z12$ axis compared with that of the analytical solution for the same problem. (b) The nine-dimensional problem; the projection of the FGFMC generated wave function (for model problem II) onto the $z12$ axis compared with that of the analytical solution for the same problem.

two uniformly, randomly distributed sets of points, with no antisymmetry, and produce many pairs of sets, each with the property that the difference of the density functions which describe the distribution of points in the pair of sets is equal to the lowest antisymmetric state. This process itself yields an estimate of the energy which, like all quantities calculated via this method, is exact in the sense that the only error is a statistical one. Such an error can be made arbitrarily small simply by carrying out the calculation for a longer time. Since the antisymmetric component is stable in magnitude, the convergence is the usual $n^{-1/2}$ for a Monte Carlo method, rather than the much slower rate $(\log n)^{-1/2}$ (see Sect. III B) obtained without the correlation methods.

The sets of points produced by the method enable other estimates of the energy, as well as of other quantities, to be made. In particular, it has been shown that by employing a reasonably good variational trial function, the error of such estimates can be dramatically reduced, without biasing the result in any way, that is without changing the exact nature of the calculation.

The FGFMC method has all but one of the properties of the standard GFMC method which makes the latter such a success. The missing quality is weak dependence on dimensionality. The key to the success of this work was the effectiveness of $G^*$ (actually $G_U^*$) in filtering out, analytically, a significant portion of the symmetric component. This could be done only when points were paired sufficiently closely, so as to maximize the quantity in Eq. (3.20). This in turn demands a certain minimum density of points in configuration space. The implication is that while the method appears to be feasible for systems of as many bodies as 10, population requirements to maintain an adequate density will make truly many-body computations impossible.

Two techniques may help overcome this problem. The first serves to reduce the effective volume of configuration space by making use of the fact that, if $r_i$, $r_j$, and $r_k$ are the positions of three identical fermions of equal spin, then the configuration space points

$$P_1 = (\ldots, r_i, \ldots, r_j, \ldots, r_k, \ldots)$$

and

$$P_2 = (\ldots, r_k, \ldots, r_i, \ldots, r_j, \ldots)$$

are in some sense, the same point. If, for another point $M_1$, a nearest neighbor point was sought in a set which contained $P_1$, and if $P_2$ was closer to $M_1$, then, regardless of whether $P_2$ was actually in the set, it would be an appropriate match for $M_1$. In other words, we change the standard euclidean distance function to one which treats the distance between two points in configuration space as the minimum euclidean distance over all even permutations of identical fermions of equal spin. Since this does serve to decrease the effective volume of configuration space, the density of points increases, overcoming, to an extent, the problem mentioned above.

The second technique which may help to overcome the density problem is importance sampling. This method, described in detail in Eq. (10), biases the random walks of points in configuration space so that they tend to take place in regions where the wave function is largest. The bias is compensated for in the calculation of estimates, so that the computation remains an exact one. Importance sampling plays a fundamental role in many-body GFMC calculations,[5] because of its variance reducing properties. Along with these properties, this technique would have the additional advantage, in the context of the FGFMC work, of concentrating configuration points in smaller regions of configuration space, thereby increasing the density of points locally. Future work in this area will apply these two techniques so as to develop a genuine many-body version of the FGFMC method.

## ACKNOWLEDGMENTS

We are indebted to D. M. Ceperley and G. V. Chester for helpful conversations and to P. A. Whitlock for a critical reading of this manuscript.

[1]M. H. Kalos, Phys. Rev. **128**, 1891 (1962). In the 1940's, Fermi and Metropolis had discussed the idea of solving partial differential equations by random walks on a lattice. See, for example, N. Metropolis, in *Symposium on Monte Carlo Methods*, edited by H. A. Meyer (Wiley Interscience, New York, 1954), pp. 29–36. At least part of the reason why these efforts didn't advance further at the time must lie in the limits of computing power then. GRMC differs from those approaches in its use of some analytically known Green's function for simulation in the continuum, rather than in a discrete lattice. The use of such a Green's function is essential for the method of this paper.

[2]M. H. Kalos, J. Comp. Phys. **1**, 127 (1966).

[3]M. H. Kalos, Nucl. Phys. A **126**, 609 (1969).

[4]M. H. Kalos, Phys. Rev. A **2**, 250 (1970).

[5]M. H. Kalos, D. Levesque, and L. Verlet, Phys. Rev. A **9**, 2178 (1974).

[6]M. H. Kalos, M. A. Lee, P. A. Whitlock, and G. V. Chester, Phys. Rev. B **24**, 115 (1981).

[7]K. Schmidt, M. H. Kalos, and M. A. Lee, Phys. Rev. Lett. **45**, 573 (1980).

[8]P. A. Whitlock and M. H. Kalos, J. Comp. Phys. **30**, 361 (1979).

[9]D. Ceperley and B. Alder, Phys. Rev. Lett. **45**, 566 (1980).

[10]D. M. Ceperley and M. H. Kalos, *Monte Carlo Methods in Statistical Physics*, edited by K. Binder (Springer, Berlin, 1979), Chap. IV.

[11]D. M. Ceperley, G. V. Chester, and M. H. Kalos, Phys. Rev. B **16**, 3081 (1977).

[12]M. H. Kalos and P. A. Whitlock, *Monte Carlo Methods* (Wiley Interscience, New York, 1983).

[13]J. B. Anderson, J. Chem. Phys. **63**, 1499 (1975).

[14]J. B. Anderson, J. Chem. Phys. **65**, 4121 (1976).

[15]J. B. Anderson, Int. J. Quantum Chem. **15**, 109 (1979).

[16]J. B. Anderson, J. Chem. Phys. **73**, 3897 (1980).

[17]M. A. Lee, K. E. Schmidt, M. H. Kalos, and G. V. Chester, Phys. Rev. Lett. **46**, 728 (1981).

[18]D. M. Arnow, Ph.D. thesis, New York University, October, 1981.